Mapping Potential Carbon Emissions from Thawing Permafrost Soils in the Yukon-Kuskokwim Delta

Ann Burr McElvein

ABSTRACT

Permafrost across the Arctic and subarctic is thawing due to climate change. This study aims to better understand carbon emissions from permafrost thaw by producing models of carbon pools and carbon lability in the subarctic Yukon-Kuskokwim delta watershed. Permafrost contains cast amounts of carbon, around 1500 petagrams. I collected soil samples in-field, tested for carbon pools and lability, then mapped carbon pools and vulnerability over various land cover classes using supervised and unsupervised classification algorithms in Google Earth Engine. Classification algorithms revealed burned areas in the region have less carbon and are less labile (2-15 kg/m² carbon pool, 0.8954-.9842 lability index) than unburned areas (20-30 kg/m² carbon pool, 1.035-1.187 lability index), and elevated, dry areas have less carbon and are less labile (4-10 kg/m² carbon pools and 0.9081-.9588 lability index) than low-lying, wet areas (25-30 kg/m² carbon pool, 1.035-1.187 lability index). This investigation revealed a relationship between carbon lability and pools across the landscape, areas of high carbon lability have high carbon pools and areas of low carbon lability have low carbon pools. Additionally, this research produced models and workflows to investigate carbon emissions from subarctic regions, which will become increasingly relevant as Arctic regions continue warming and become increasingly similar to subarctic regions in permafrost thaw.

KEYWORDS

Climate change, carbon lability, microbial emissions, remote sensing, classification algorithm.

INTRODUCTION

Permafrost occupies about 26% of the total exposed land surface in the Northern Hemisphere, 16% globally, and sequesters 1672 petagrams of carbon, which is estimated to be half of the global belowground organic carbon pool and about two times the global atmospheric carbon level (Zhang et al. 2003, Tarnocai et al. 2009). Carbon gas emissions from thawing permafrost are therefore incredibly significant for global climate change, as there is such a vast amount of carbon potentially emitted during warming. As permafrost soils thaw, indigenous microbes become more active and more organic compounds become available, resulting in increased consumption and carbon emission (Schuur et al. 2008, Jansson and Taş 2014). In permafrost soils, microbes turn complex organic compounds to soluble metabolites and gases, including carbon dioxide, methane and nitrous oxide (Graham et al. 2011). The likelihood that a microbe consumes organic soil carbon and emits gas is known as the soil lability. Labile carbon is usually found in organic soil rich with simple carbohydrates and amino acids (Zou et al. 2005). The released microbial gasses from labile carbon are primarily greenhouse gasses, meaning their presence in Earth's atmosphere contributes to global climate change. Therefore, quantifying the gas emissions from microbes in thawing permafrost is crucial for understanding global climate change. The Yukon-Kuskokwim delta is specifically important to model because it is an area of subarctic permafrost, and as the Arctic continues to warm, vast regions of carbon-heavy Arctic permafrost will start emitting carbon in patterns characteristic of subarctic permafrost (Nitze et al. 2019).

The area of permafrost investigated is the Yukon-Kuskokwim delta; a topographically varied region with patterns of different elevations and wildfire burn scars. The
Yukon-Kuskokwim delta watershed is a region of sporadic permafrost, meaning the ground is intermittently permafrost and thawed soil, which impacts the regional elevation. Presence of permafrost controls the elevation in the region, lower areas are wet regions of thaw while higher areas are drier with a thicker permafrost layer (Jorgenson and Ely 2001). In addition to the elevation change, the Yukon-Kuskokwim delta has regions of unburned soil and burn scarring from wildfires in 2015 and 1972 (Michaelides et al. 2019). The topographical elevation and moisture differences are known to decrease decomposition of organic matter, and burning is known

reduce available carbon (Schuur et al. 2008, Wild et al. 2014). Therefore, the elevation and burn patterning can be used in developing a relationship between the Yukon-Kuskokwim delta landscape and carbon emissions.

Remote sensing technology can be employed to better understand the topography and associated emissions of the delta. As the Yukon-Kuskokwim delta can be broken down into a variety of distinct land cover types based on burning and elevation, this area lends itself well to remote sensing-based analysis. In 2018, a team of investigators successfully classified a coastal region of the Yukon-Kuskokwim delta into 8 ecotypes based on topography, vegetative cover, and water cover, demonstrating the area's aptitude for remote sensing analysis (Whitley et al. 2018). The distinct soil classes used for analysis in this investigation are purposefully similar to the land classes used in the Whitley investigation.

The objectives of this investigation are to collect samples and calculate the carbon lability and pool by volume of each soil sample, assess the validity of the land classes, and model the spatial relationship between soil carbon and the landscape. The information generated can be used to predict carbon emissions, with the goal of ultimately contributing to global climate change models, which currently do not incorporate detailed models from regions of permafrost thaw (Gray 2018, Graham et al. 2011).

METHODS

Study site

The Yukon-Kuskokwim delta (YKD) watershed is about 129,500 square kilometers of subarctic tundra that lies 40 miles west of Bethel, Alaska. The center of the watershed can be found at longitude: -163.25, latitude: 61.26. The YKD has a mix of high and low elevation areas that loosely coincide with sporadic permafrost thaw. The depth and presence of frozen permafrost varies throughout the region (Jorgenson and Ely 2001). Permafrost is rigid, frozen soil that adds structure to the landscape, when it thaws the ground slumps lower because of the lost support (Zhang et al. 2003). While the ground slumpls lower, water from thawed permafrost percolates to

the surface forming wetlands called fens or lakes called thermokartst (Sui et al. 2018). In the YKD, low areas are wet and high areas are dry, so this investigation conflates elevation with moisture.

In addition to permafrost variation controlling elevation, there is variation in burned areas of the landscape from wildfires. The YKD was burned by wildfires in 2015 and 1972, and the scarring is still visible by satellite (Michaelides et al. 2019, Fiske 2017). Those burned regions, in combination with the sporadic permafrost thaw and wetland formation, are typical of subarctic permafrost (Zhang et al. 2003). The distinct elevation and burning features create interesting variations in topography and moisture in the YKD that are classifiable through a combination of fieldwork and remote sensing.

Preliminary land class establishment

To segment the YKD into different land classes representative of the region, I visited the field sites and visually interpreted the landscape to discern distinct land cover types. The classes I identified are high and dry unburnt, high and dry burnt, low and wet unburnt, and low and wet burnt. These four classes account for the burn variation and wetness variation indicative of permafrost thaw (Michaelides et al. 2019, Jorgenson and Ely 2001). Broad land classes were needed to structure sample collection and were validated after collection and processing.

Soil sample collection

To obtain information about the carbon pools and vulnerability within the different land cover classes, I collected numerous soil samples from each class. I collected the samples by coring the active layer using a modified hand drill. Each core was approximately 30 centimeters deep and 6 centimeters in diameter (Figure 1). At each site that represented one of the four land cover classes, I collected between 3 and 6 soil samples. Each land cover class had at least 3 sites sampled in 2018, for a total of 150 sample points in 2018, and an additional 150 archived and geotagged samples collected by former researchers in 2017 were also included. The soil samples from 2017 were not from the same sites as 2018, but they were from the same landscape, so I assigned them

to the 4 land class categories. Each sample I collected was geotagged and recorded to track the area and land class from which it was taken.

Figure 1. **Demonstration of an active layer core**. Photo of author by John Schade during 2018 YKD expedition.

Carbon pool per volume

To determine carbon pool, I first homogenized, subsampled and dried each soil sample in 60° Celsius ovens and ground them using a SPEX High-Energy Ball Mill. The proportion of carbon for each ground, dried soil sample was determined using a LECO elemental analyzer.
Then carbon pools in per soil volume for each sample were calculated using the formula:

(*proportion C from LECO analyzer*)(*dry soil mass in grams*) (*soil volume in* m^3)(*sampling depth in m*) .

Carbon lability

To calculate carbon lability, I first obtained the spectral profile of each of my samples using a Fourier-transform infrared spectroscopy machine. I then used the ChemoSpec package in R version 5.0.88 to calculate a metric of lability (Hansen 2018, R Core Team 2018). The lability calculation is a ratio of aromatic to carboxylic peaks in each sample (Ernakovich et al. 2015). Figure 2 illustrates the peaks I used in an example spectrum.

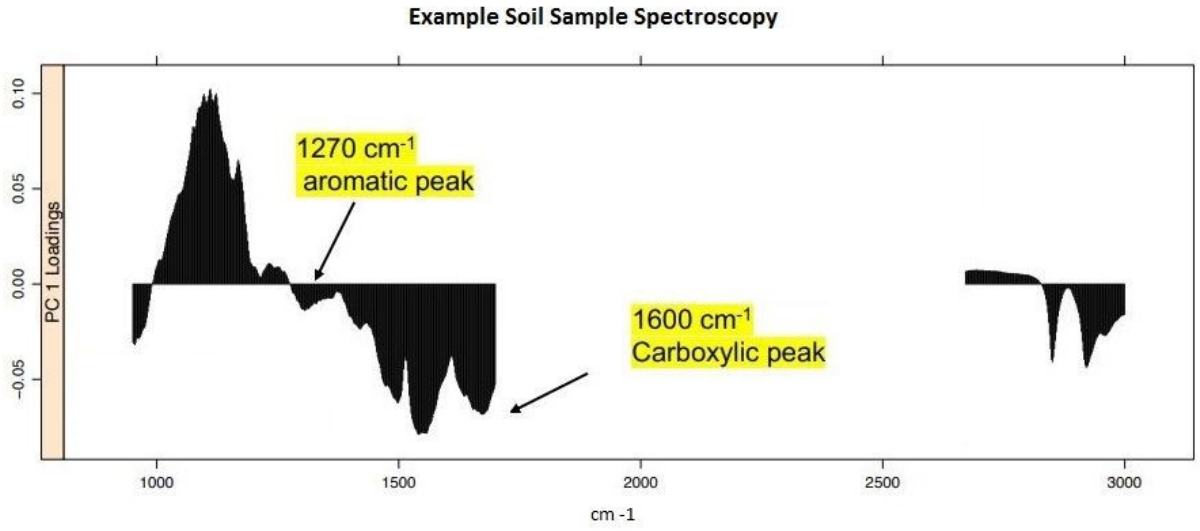

Figure 2. Reference spectrum. The proxy for carbon lability was determined by the ratio of aromatic to carboxylic peaks.

Land class validation

After collecting soil samples from each of the land classes and calculating the carbon pool and lability figures for each of the samples, I had sufficient data to validate the land classes. I began the validation by comparing percent carbon and lability by land cover class. That information suggested accurate land cover classes, and I confirmed that suggestion by conducting a robust PCA in R version 5.0.88. I further proved statistical significance with an ANOSIM (R Core Team 2018).

Mapping and modeling

I then segmented raster imagery from the Landsat 6 Arctic DEM satellite into each land cover class using an supervised classification algorithm (ee.Clusterer) in Google Earth Engine and incorporated Sentinel 2 multispectral imagery (Gorelick et al. 2017). The resolution was limited to the Landsat dataset resolution of 5 meters. I incorporated Gregory Fiske's 2017 unsupervised classification map of the region to validate the land cover classes, and later trained that map using 30% of the field-collected points (Fiske 2017). The satellite imagery was filtered to 2016-2017, summer, cloud free days. Derived products included as covariates were NDVI, NDWI, and slope. This remote-sensing analysis produced refined maps of the distribution of carbon pools and lability.

RESULTS

Soil organic carbon pools and carbon lability

Percent soil organic carbon and carbon lability differed for each land cover class. Low, wet areas contained more percent carbon and a higher carbon lability index, while burned plateau areas had less percent carbon and a lower carbon lability index. The percent carbon for the two burned regions, 2015 and 1972, was ~37% (Figure 3). The percent carbon per land cover class bar graph revealed only moderate differences, but the lability bar graph revealed unburned and fen areas were about 15% more labile than both the 2015 and 1972 burned areas. These differences in carbon lability justified the further robust principal component analysis.

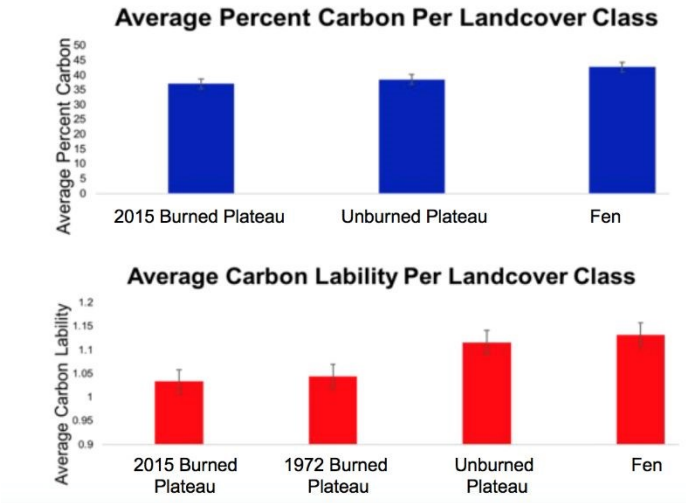

Figure 3. Percent carbon and carbon lability by land cover class. Average percent carbon analysis was conducted on samples from 2018, average carbon analysis was on samples from 2016, 2017, and 2018.

Validating land classes

The robust principal components analysis revealed differences by land cover class. The first three components in the robust PCA explained 96% of variation in the data, with the first component alone explaining 78% (Figure 4). Additionally, the first two components in the robust PCA explained 85.4% of the total variation in the soil data. The significance of the similarities between samples in each class was validated with a one-way ANOSIM, producing an R-value of .4 and an associated p-value of 0.001 between land cover classes.

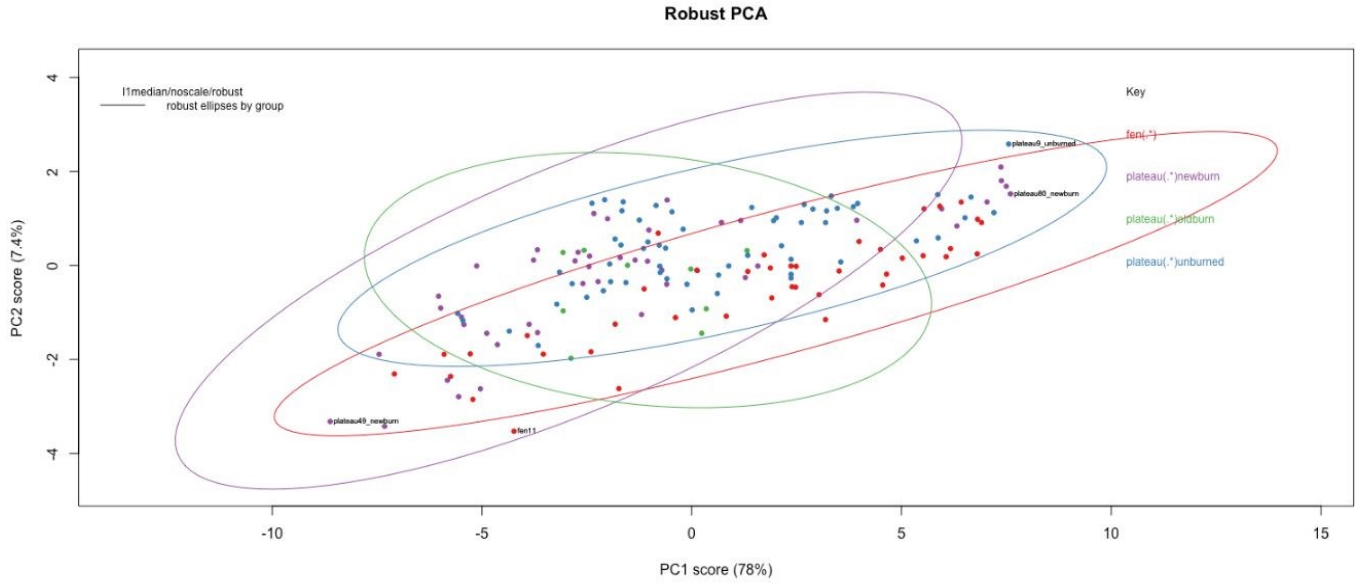

Figure 4. Robust PCA of soil samples from land cover classes. Inputs were full spectra.

Mapping pools and lability across the landscape

Wildfire burns corresponds to a decrease in carbon pools and lability and lower, wetter areas correspond to an increase in carbon pools and lability. Burned areas had carbon pool values in the range of 2-15 kg/m² and lability index values in the range of 0.8954-.9842. Unburned areas had carbon pool values in the range of 20-30 kg/m² and lability index values in the range of 1.035-1.187. High, dry areas had carbon pool values in the range of 4-10 kg/m² and lability index values in the range of 0.9081-.9588, while low, wet areas had carbon pool values in the range of 25-30 kg/m² and carbon lability values in the range of 1.035-1.187.

Carbon lability and carbon pools reflect similar patterning across the delta. Where there is high carbon lability, there are large carbon pools and where there is low carbon lability, there are smaller carbon pools. This direct relationship corresponds to the locations of wetlands and wildfires; burnt areas have low carbon lability and low carbon pool, wet areas have high carbon lability and high carbon pool. The accuracy of these maps was validated with confusion matrices in Google Earth Engine calculated to be within 5 meters.

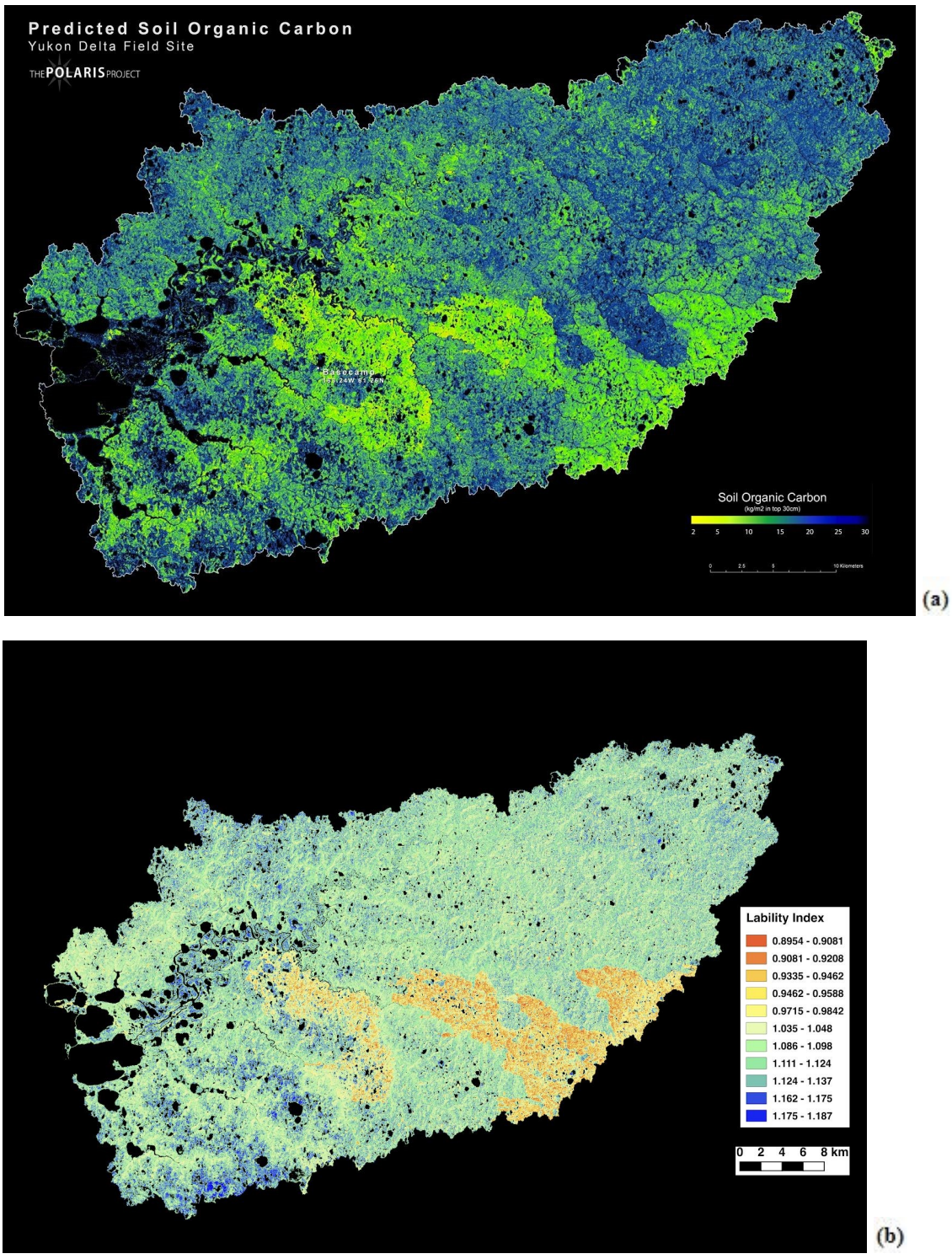

Figure 5. Predicted (a) soil organic carbon pools and (b) carbon lability. Carbon pool map made from 2016, 2017, and 2018 data. Green/yellow areas are burned and/or elevated. Carbon lability map made from 2018 data, orange/red areas are burned and/or elevated.

DISCUSSION

This investigation was successful in its objectives. I determined soil carbon profiles for each sample collected in the YKD by calculating carbon pools and lability, assessed the validity of the land classes chosen, and mapped the carbon pools and lability across the watershed. This investigation found that carbon pools and lability are lower in burned areas and higher in wetter areas, which is supported by literature. Additionally, the land classes used in mapping were statistically significant (R=.4). The maps produced with soil samples and land classes clearly model carbon pools and lability across the landscape and can be used together to predict potential carbon emissions. Satisfaction of these objectives allows for improved understanding of carbon emissions in the YKD.

Carbon profiles of soil samples

Comparing the carbon pools and lability I calculated at each sample point reveals the carbon distribution over the landscape. Carbon pools and lability are low in burned and topographically elevated areas, and high in unburned and topographically lower aeras. These results are generally consistent with published literature (Jorgenson and Ely 2001, Michaelides et al. 2019). My carbon pools and lability measurements were lower than anticipated because of my sampling method, which involved only sampling the top 30 centimeters of the soil. Carbon pools and lability are low in the topsoil of burned areas (about one class lower than unburned areas) because burning converts organic, labile carbon to recalcitrant char and depletes carbon pools (Michaelides et al. 2019). The relatively shallow cores explain why the burn sites had particularly low carbon lability and pool calculations. The labile carbon was burnt off leaving recalcitrant carbon and char behind. Sampling the entire soil column would raise the carbon lability and pool values and minimize the difference between burned and unburned areas.

Additionally, my carbon lability measurements depended on a inexact calculation and there are associated errors. The Ernakovich ratio is a rough metric of carbon lability in permafrost soils (Ernakovich et al. 2015). The ratio works well in organic soils but the peaks required to calculate a lability metric can get obscured with noise in soils that are highly inorganic. Wet soils are more

inorganic than dry soils, so the Ernakovich ratio was more successful in dry areas than wet (Tarnocai et al. 2009). This inconsistency in producing a carbon lability measurement could have caused the wet areas to have a larger margin of error than dry areas. Despite its faults, other proxy ratios were not as effective in permafrost soils because of the carboxylate distribution (Martens et al. 1992). The Ernakovich ratio was developed in soils similar to YKD soils and was the best published option for lability calculations.

Land cover class validation

Soil carbon characteristics are largely consistent within individual study sites, as demonstrated by the PCA and ANOSIM. Figure 3 demonstrates variability in the samples, but only uses the samples from 2018 with 3 classes, so no statistical conclusions can be drawn. Although not robust enough to stand alone, that preliminary analysis was promising and justified running a PCA to further investigate, especially because the findings in figure 3 are supported by literature such as the 2019 Michaelides et al paper. The PCA corroborates the previous body of knowledge and determined the land classes and associated soils are clustered together in significantly similar ways. To validate the PCA and test for significance in similarities between samples of each class, I ran a one-way analysis of similarities (ANOSIM), which produced an R-value of =.4 and an associated p-value of 0.001. An R-value of 1 indicates that the most similars soil samples are all within the same site and an R-value of 0 indicates the distribution is random. An R-value of .4 is generally low, but it is statistically significant for Arctic soil research (Wild et al. 2014). All soils are chemically very similar, and soils from the same region are even more similar to the point of lowering confidence in significant differences, resulting in a lower R-value (Lee et al. 2011). An R value of .4 is moderately significant for most soils, highly significant in terms of Arctic soils, which tend to be particularly similar due to slow turnover rate (Wild et al. 2014).

Mapping and modeling

The product of my research is two maps, one with a distribution of carbon lability and one with a distribution of carbon pools. There must be carbon present for microbes to consume, and the carbon must be in a labile form. (Gray 2018, Jansson and Taş 2014). The maps displayed similar contours in carbon lability and carbon pools, which follow the burn and elevation contours of the landscape, visually validating the current understanding of the relationship between Arctic carbon and topography (Michaelides et al. 2019, Jorgenson and Ely 2001). Wildfires influence carbon distribution by converting labile carbon to recalcitrant carbon and by diminishing carbon pools during the burning process, which is why the burned areas had lower carbon lability and pool metrics (Michaelides et al. 2019). Low-lying areas are formed when permafrost thaws, the ground slumps, and marshy wetlands and lakes form. Those areas are full of fresh, organic, labile carbon, which is why the lower elevation areas had higher carbon pool and lability metrics (Jorgenson and Ely 2001, Sui et al. 2018).

The classification algorithm and a random tree generation in Google Earth Engine used to make the maps are industry standards. The maps have an accuracy of 5 meters as calculated by a confusion matrix in Google Earth Engine which is limited by the resolution of the Landsat 6 imagery used and is a common granularity for remote sensing analyses (Gorelick et al. 2017, Fiske 2017, Whitley et al. 2018).

Limitations and future directions

Part of the merit of this project was the small scale of it, which allowed for accuracy in the training points and model validation but limited the scope of the research. Remote sensing approaches are generally only successful in the areas in which they are trained (Whitley et al. 2018). This model is built and trained on points sampled in the Yukon-Kuskokwim delta so future attempts to include more points and broaden it to vastly areas might not be accurate. Additionally, my models are structured around the patterning of elevation and wildfires in the

YKD, so my workflow will not be useful if used in a region without those characteristics because of how integral burns and elevation are to the landscape (Michaelides et al. 2019, Jorgenson and Ely 2001). However, this paper can be used to guide and plan similar arctic research, and the modeling can be used in other areas with elevation and burn patterning if the YKD sample points are discarded and new sample points from a different area are used as inputs.

Another limitation in my work is the absence of water classes. Arctic lakes are a crucial component of climate change, in their carbon emission contributions and their response to warming (Nitze et al. 2017). Lakes are also a defining feature of permafrost regions and neglecting to include them can reduce the land cover studied by as much as 50% (Sui et al. 2018, Jorgenson and Ely 2001). When I began this investigation, I sampled sediments from different lake classes in addition to my soil samples, with the intention of including them in my maps. However, modeling the lakes proved to be difficult because they contain more inorganic components than soils which caused the Ernakovich ratio to fail (Ernakovich et al. 2015). Future work could be done to include sediment carbon information, maybe by developing a more robust calculation for carbon lability, which would produce a more comprehensive model of the Yukon-Kuskokwim watershed.

Broader implications

This research quantifies and maps factors that define potential emissions in the Yukon-Kuskokwim delta. As the climate continues to warm and the permafrost continues to thaw, ground collapse will increase wetland formation and extreme weather patterns will increase wildfire burning, meaning more Arctic areas will start emitting carbon in patterns similar to the YKD. These maps, when used in conjunction, can forecast carbon emissions from each land cover class, because predicted emissions depend on a combination of pools and lability. The analysis and workflow outlined in this paper can be used to map future Arctic or subarctic potential carbon emissions, and the results can be incorporated into global permafrost models.

Permafrost isn't usually accounted for in climate models so this research, and research like it, is critical. Excessive amounts of carbon from regions of permafrost thaw will contribute staggering amounts of carbon gas to our atmosphere, which will lead to the positive feedback loop

of increased climate change and increased permafrost thaw. We need to know what our carbon sources will be as our world heats up past a point of no return.

ACKNOWLEDGEMENTS

Thank you so much to all of the wonderful people I've gotten to know through creating this project: Susan Natali, John Schade, Paul Mann, Seeta Sistla, Sarah Ludda Ludwig, Greg Fiske, Aiyu Zheng, Margaret Powell, Kelly Turner, Mia Arvizu, Darcy Peter, Rhys MacArthur-Thompson, Alexandra Lehman, Natalie Baillargeon, Joshua Reyes, Jordan Jimmie, Nathaniel Mann, Kevin Pettway, and Robin Carroccia. Without you all I would be dead in the tundra. Special thank you to Tina Mendez, Kurt Spreyer, Leslie McGinnis, Ellen Plane and the rest of the 175 class for all of your assistance and input in shaping this project. This research benefited from the support and services of the UC Berkeley Geospatial Innovation Facility (GIF), gif.berkeley.edu, UC Berkeley's College of Natural Resources Travel Grant, and funding from NSF for the Polaris Project (NSF21624927).

REFERENCES

Ernakovich, J. G., M. D. Wallenstein, and F. Calderón. 2015. Chemical Indicators of Cryoturbation and Microbial Processing throughout an Alaskan Permafrost Soil Depth Profile. Soil Science Society of America Journal 79:783.

Fiske, G. (2017). Unsupervised Classification Map of Yukon-Kuskokwim Delta [Map]. Unpublished.

Graham, D. E., M. D. Wallenstein, T. A. Vishnivetskaya, M. P. Waldrop, T. J. Phelps, S. M. Pfiffner, T. C. Onstott, L. G. Whyte, E. M. Rivkina, D. A. Gilichinsky, D. A. Elias, R. Mackelprang, N. C. VerBerkmoes, R. L. Hettich, D. Wagner, S. D. Wullschleger, J. K. Jansson. 2011. Microbes in thawing permafrost: The unknown variable in the climate change equation. The ISME Journal 6:709-712.

Gray, E. (2018, August 20). Unexpected future boost of methane possible from Arctic permafrost – Climate Change: Vital Signs of the Planet. Retrieved from https://climate.nasa.gov/news/2785/unexpected-future-boost-of-methane-possible-from-Arctic-p ermafrost/.

Gorelick, N., Hancher, M., Dixon, M., Ilyushchenko, S., Thau, D., & Moore, R. (2017). Google Earth Engine: Planetary-scale geospatial analysis for everyone. Remote Sensing of Environment.

Hansen, B., (2018). *ChemoSpec: Exploratory Chemometrics for Spectroscopy*. R package version 5.0.88. https://cran.r-project.org/web/packages/ChemoSpec/index.html.

Jansson, J. K., and N. Taş. 2014. The microbial ecology of permafrost. Nature Reviews Microbiology 12:414–425.

Jorgenson, T., and C. Ely. 2001. Topography and flooding of coastal ecosystems on the Yukon-Kuskokwim delta, Alaska: Implications for sea-level rise. Journal of Coastal Research 17:124-136.

Lee, C. K., B. A. Barbier, E. M. Bottos, I. R. Mcdonald, and S. C. Cary. 2011. The Inter-Valley Soil Comparative Survey: the ecology of Dry Valley edaphic microbial communities. The ISME Journal 6:1046–1057.

Martens, C. S., C. A. Kelley, J. P. Chanton, & W. J. Showers. 1992. Carbon and hydrogen isotopic characterization of methane from wetlands and lakes of the Yukon-Kuskokwim delta, western Alaska. Journal of Geophysical Research 97:166-189.

Michaelides, R. J., Schaefer, K., Zebker, H. A., Parsekian, A., Liu, L., Chen, J., . . . Schaefer, S. R. (2019). Inference of the impact of wildfire on permafrost and active layer thickness in a discontinuous permafrost region using the remotely sensed active layer thickness (ReSALT) algorithm. *Environmental Research Letters, 14*(3), 035007.

Nitze, I., G. Grosse, B. Jones, C. Arp, M. Ulrich, A. Fedorov, and A. Veremeeva. 2017. Landsat-Based Trend Analysis of Lake Dynamics across Northern Permafrost Regions. Remote Sensing 9:640.

Nitze, I., G. Grosse, B. M. Jones, V. E. Romanovsky, and J. Boike. 2019. Remote sensing quantifies widespread abundance of permafrost region disturbances across the Arctic and subarctic. Nature Communications 10.

R Development Core Team. 2018. R: A language and environment for statistical computing. R Foundation for Statistical Computing, Vienna, Austria. http://www.R-project.org/.

Schade, J. (2018). Soil core [Photograph]. Yukon-Kuskokwim Delta, Alaska.

Schuur, E. A., J. Bockheim, J. G. Canadell, E. Euskirchen, C. B. Field, S. V. Goryachkin, S. Hagemann, P. Kuhry, P. M. Lafleur, H. Lee, G. Mazhitova, F. E. Nelson, A. Rinke, V. E. Romanovsky, N. Shiklomanov, C. Tarnocai, S. Venevsky, J. G. Vogel, S. A. Zimov. 2008. Vulnerability of permafrost carbon to climate change: Implications for the global carbon cycle. BioScience 58:701-714.

Sui, Y., D. Fu, X. Wang, and F. Su. 2018. Surface Water Dynamics in the North America Arctic Based on 2000–2016 Landsat Data. Water 10:824.

Tarnocai, C., J. G. Canadell, E. A. G. Schuur, P. Kuhry, G. Mazhitova, S. Zimov. 2009. Soil organic carbon pools in the northern circumpolar permafrost region. Global Biogeochemical Cycles 23:2023-2034.

Whitley, M., G. Frost, M. Jorgenson, M. Macander, C. Maio, and S. Winder. 2018. Assessment of LiDAR and spectral techniques for high-resolution mapping of sporadic permafrost on the Yukon-Kuskokwim delta, Alaska. Remote Sensing 10:258-267.

Wild, B., J. Schnecker, R. E. Alves, P. Barsukov, J. Bárta, P. Čapek, N. Gentsch, A. Gittel, G. Guggenberger, N. Lashchinskiy, R. Mikutta, O. Rusalimova, H. Šantrůčková, O. Shibistova, T. Urich, M. Watzka, G. Zrazhevskaya, A. Richter. 2014. Input of easily available organic C and N stimulates microbial decomposition of soil organic matter in Arctic permafrost soil. Soil Biology and Biochemistry 75:143–151.

Zhang, T., R. G. Barry, K. Knowles, F. Ling, R. L. Armstrong. 2003. Distribution of seasonally and perennially frozen ground in the Northern Hemisphere. Permafrost: Proceedings of the 8th International Conference on Permafrost, Zurich, Switzerland 1:1289-1294.

Zou, X., Ruan, H., Fu, Y., Yang, X., & Sha, L. (2005). Estimating soil labile organic carbon and potential turnover rates using a sequential fumigation–incubation procedure. *Soil Biology and Biochemistry, 37*(10), 1923-1928.